**PROCEEDINGS OF THE INTERNATIONAL CONFERENCE ON NEWVIEWS IN ENGINEERING AND TECHNOLOGY (ICNET) MAIDEN EDITION, FACULTY OF ENGINEERING, RIVERS STATE UNIVERSITY, PORT HARCOURT, NIGERIA.**
**27th October 2021**
**Available online at** https://conference.rsujnet.org/

**Paper number: ICNET2021-015**

# FPSO Hull Corrosion Management to Minimize Operational Down-Time Due to Artificial Metocean Conditions: A Thermal Approach

**Charles, Watiminyo James[1], Izionworu, Vincent Onuegbu[2]; Orji Charles U. [1]**
1 Department of Marin Engineering, Faculty of Engineering, Rivers State University, Nkpolu-Oroworukwo, Port Harcourt, River State.
2 Department of Chemical/Petrochemical Engineering, Faculty of Engineering, Rivers State University, Nkpolu-Oroworukwo, Port Harcourt, River State.
**Corresponding author's email: vincent.izionworu@ust.edu.ng; barawatiminyo@yahoo.com**

## ABSTRACT

*It is not uncommon to find a less than 3% coating breakdown in the first 2 to 3 years of operation among FPSOs operating world-wide having hulls with conventional coatings ($C_c$). Two different coatings $S_1$ and $S_2$ formulated from an aggregate of paints shall be investigated along-side the conventional coating by means of factorial experiment, pull test, GCMS and Holiday test in order to ascertain the superiority of $S_1$ and $S_2$ to $C_c$. Thermal radiation values of 3.9Kw/m$^2$ and 4.1Kw/m$^2$ were simulated from two flare stacks operating at 3.5 bara and 1.5 bara respectively using DNV PHAST software. Temperature conversions from these thermal radiation values using Stefan Boltzman's equation yielded 123.85$^0$C and 102.43$^0$C. These temperatures, salinity of 55.25ppt and Ph of 7.52 will be combined to treat twenty-four (24) carbon steel coupons coated with the three coatings. The main effects from the factorial experiment and the pull test will be reported. Gas Chromatography Mass Spectrometry will be used to study the degradation of the coating layers over time of immersion in the saline environment at the different temperatures123.85 $^0$C and 102.43 $^0$C while Holiday test will be conducted to determine any discontinuity in the coatings. The ability of $S_1$ and $S_2$ to overcome the 3% coating breakdown problem will be examined using Anova and the best option adopted as FPSO coating against corrosion in saline environment under elevated temperature.*

**KEYWORDS:** FPSO Hull, Artificial Metocean, Thermal radiation, Vessel, Corrosion.

**Cite This Paper**: Charles, W. J., Izionworu, V. O., & Orji C. U. (2021). FPSO Hull Corrosion Management to Minimize Operational Down-Time Due to Artificial Metocean Conditions: A Thermal Approach. *Proceedings of the International Conference on Newviews in Engineering and Technology Maiden Edition*, Faculty of Engineering, Rivers State University, Port Harcourt. Nigeria, 27th October 2021, ICNET2021-022, 228 – 241.

## 1. INTRODUCTION:

All over the world, oil and gas exploration is faced with the challenge of fields in very deep-water depths and uneconomical reserves with little or no profitable drive for exploitation by conventional fixed platform approaches (John, 2013). The choice and decision of the type of production process to be used is therefore dependent on several factors which amongst others include Location of a Field and the size, its water depth, ocean currents and how harsh the weather is. The best option for production purposes will hence not be a fixed installation following technical considerations given the challenges mentioned above. A floating unit would offer the best economic advantage (Pike, 1999).

It is these challenges that necessitated the use of Floating Production, Storage and Offloading systems (FPSOs) since the mid-1970’s in the offshore oil and gas production. FPSO’s have proved to be quite beneficial and economical over fixed production platforms especially when production is in remote deep-water locations or where it is difficult to install export pipelines and run them over time. The mobility of FPSO’s is an amazing fit as they can be floated off at the end of a field’s productive life to another production field or location with great economic benefits such as a saved cost of facility fabrication etc. This economic advantaged becomes pronounced for marginal fields that have a short life span with production facilities required for only a few years (John, 2013).

Complex engineering drivers are usually engaged when a selection of an FPSO concept properly suited for a specific field development is required. To meet the demand for a FPSOs it has become a common practice for oil tankers used for product delivery to be converted to an FPSO in the offshore oil and gas industry. A major driver of this initiative is the usually lower capital expenditure involved in the fabrication that converts a tank to an FPSO. Again, this possibility that has been exploited as was the case in the Gulf of Mexico (Ozgur, 2020) helps industry players to meet tight schedule. As a requirement some basic considerations are made during an oil tanker design, these design considerations such as speed, low fuel consumption and carrying capacity are essentially what makes them suitable for conversion into FPSO’s. Also, the remaining fatigue life left and that spent, and the trading route are important factors (Ozgur, 2020; John, 2013). To achieve speed and fuel economy, tankers are designed to have large length/beam (L.B) ratios with comparatively slender hull forms.

The design considerations of an FPSO implemented in the FPSO construction is such they remain stationary at a location over a period of time bearing the designed storage capacity and yet support a large topside payload during downtime in production. The structural integrity of an FPSO hull usually have weighty effect on both production plant Non-Productive Time (NPT) and the mooring and riser systems. Any financial advantage associated with conversion of a tank to an FPSO or the outright construction of a new FPSO can be speedily lost if the FPSO hull designed fails to address specific field environmental concerns embodied in the condition of the area. This kind of neglect in design leads to frequent shutdowns with the associated issues of loss of production or high cost of mooring and riser systems repairs. A crucial design consideration during selection of the type of FPSO hull is the effect of the site-specific met ocean conditions on the hull integrity and capacity to withstand degradation and failure of the coating system used on the hull to minimize production downtime resulting from parent material of construction damage. (John, 2013)

During construction phases in FPSO projects, several materials are usually selected to protect the material of construction for the hull from the hostile ocean environment. Some of these materials include marine Epoxy (Aluminum), marine Epoxy (Bronze), Epoxy Tie-Coat (Gray), slow polishing A-F (Red) etc. Any of the established methods could be used to select a suitable material to protect the hull if the ocean water temperature at the site is considered without any recourse to the additional temperature factor generated by the presence of the flare system. However, an artificial met ocean condition is created by the flare system on the main deck of any FPSO. The severity of this artificial condition depends on factors such as solar radiation, the pressure regime of the flare system, condition of the flared gas (wet or dry) etc (Buchi, 2010). This artificial ocean condition has the potential of damaging the hull faster than the traditional environment. This study investigates the situation to find the best material to protect hulls of FPSO in the Gulf of Guinea.

It has already been established that it is common to find less than 3% coating breakdown in the first 2 to 3 years of operation among FPSOs operating world-wide (Adrian et al., 2004). It is also proven that a rise in temperature to about $10^0$C when other conditions are constant can double the rate of corrosion (Adrian *et al.*, 2004). When these two conditions combine in any situation, it could double the corrosion rate in the hull of an FPSO. The artificial metocean condition created by the thermal radiation from the flare stack is a catalyst for speeding up the rate of corrosion leading to operational down time and huge financial losses. As a solution to listed problem in the preceding paragraph, this paper shall present both experimental and analytical methodologies to establish the artificial metocean condition proximate to the FPSO hull and use the information to manage the design of the hull in a manner that it shall not fail before expected design life in order to prevent operational down time.
A brief literature review relating to the study shall follow in the subsequent paragraphs addressing software, metocean design data, corrosion, and FPSO hull coating design.

**A jet** flame occurs following the ignition and combustion of a flammable fluid issuing continuously from a pipe or orifice, which burns close to its release plane (Chamberlain, 1987). Releases that fuel jet fires could be accidental or intentional. An example of the latter are jet flames from flare systems of offshore oil and gas production facilities, which are primarily operated to provide a safe means of disposal of hydrocarbon gas under a variety of process conditions. Jet flames dissipate thermal radiation, which, away from the flames visible boundaries, transmit heat energy that could be hazardous to life and property. Thus, in the evaluation of the hazard posed by jet flames, the accurate determination of the likelihood of flame impingement and/or the amount of radiant energy received by objects at a distance from the flame is of primary importance.

Models developed for estimating the received radiated heat flux by objects at a distance from jet flames can he divided broadly into three categories. These are: Semi-empirical, Field, and Integral models. Semi-empirical models are relatively simple and are usually designed to predict quantities such as flame shape and heat fluxes to external objects without providing a detailed description of the fire itself. They can be further divided into: point source, multiple point source and surface emitter models. Point source models do not attempt any shape prediction and represent the source of heat radiation by a point (e.g., API-521 model). On the other hand, multiple point source models attempt to model the effect of flame shape on radiated heat flux by representing the flame with a flame Centre line trajectory along which several radiating point sources are distributed. Surface emitter models represent the flame by a solid object (usually a cone or a cylinder) from which heat is being radiated.

Field models are formulated on solutions of the time-averaged Navier-Stokes-equations for conservation of mass, momentum and other scalar quantities in a flowing fluid (Chamberlain, 1987). Field models require additional sub-models in order to adequately describe important physical and chemical processes taking place during the combustion of a flowing fluid. They are mathematically complex, requiring a lot of effort in coding and expend significant run times on high performance computer systems.

Integral models are a compromise between semi-empirical and field models. In these models, with the aid of simplifying assumptions, the partial differential equations coupled with the sub-models in field models are reduced to ordinary differential equations and subsequently integrated. They are less rigorous and less computationally expensive when compared with Field models. Of the three modelling categories described above, semi-empirical models are the most attractive with respect to hazard assessment purposes. In comparison with integral or field models, semi-empirical models are mathematically simpler, easier to understand and formulate, quicker to implement in computer programs require significantly shorter computational run times and predict flame properties that are of interest to hazard assessment studies with reasonable accuracy. However, semi-empirical models are heavily dependent on experimental data, and are limited to the specific type of fire studied during experimentation and the range of conditions under which model correlations were derived.

In all, several semi-empirical models exist for jet fire modelling that have been correlated over a wide range of conditions encompassing typical jet fires encountered in reality. Of these, the basic features of the surface emitter model by Chamberlain, which was later extended by (Johnson *et al.*, l994), have been adopted and implemented in the JFSH model. This model forms the basis on which the Process Hazards Analysis Software Tool (PHAST) is founded.

The site-specific metocean conditions at a particular location have a great influence on operability and availability of a spread moored FPSO (Jinzhu, 2012). In the design of the FPSO topsides and hull structures, as well as the design and selection of the process systems and equipment, designers must use site-specific metocean data. The topsides, utilities, and offloading system will all have availability based on the calculated operational windows based on the site-specific wind, wave, and current conditions' joint probability distributions. The overall facility availability is the joint availability of all systems, equipment, and personnel on board.

The hull and topsides systems and equipment should be developed to project specific FPSO motion criteria in an iterative manner, irrespective of all severe and unique metocean conditions. A high availability target increases the difficulty to meet motion standards in the design of systems equipment and the hull designer for a low-motion hull configuration. To establish a realistic balance between expected hull motion and topsides availability, a multi-disciplinary approach is necessary. (Xia, 2013).

The hull and topsides systems and equipment should be tailored to project specific FPSO predicted performance regardless of the severity of specific metocean conditions. (Xia, 2013).

The main design objectives for the operational metocean conditions are twofold. The first is to minimize the probability of vessel motion exceedance for greater windows of process plant operation, offloading operation, crew habitability and helicopter operation. Secondly, to minimize the cumulative motion probability distributions for minimal structural, riser and mooring fatigue.

Mooring fatigue requires attention because of the associated consequence if it fails. Studies have shown that mooring systems have badly affected by corrosion that exceeded the Classification or Class Societies corrosion allowance at the time at the range of 0.4 mm/y on each surface (Melchers *et al.*, 2012).

The first step in the design is to identify the metocean condition the FPSO is exposed to. required natural periods of roll and heave. Pitch natural period is generally 1 or 2 seconds below heave natural period for shipshape FPSO and is less critical due to high damping. The required natural periods of roll and heave are determined from the field environmental data (Jinzhu, 2012).

Corrosion allowances for traditional ship designs are based on 10-year service and are provided in various classification society standards, e.g. DNV Rules for ships (Adrian et al., 2004)

Utilizing the corrosion rates given in Table 1, the general ballast tank corrosion allowance will be in the range from 1mm to 3.5mm for one sided corrosion exposures. For members with two sided corrosion exposure the corrosion allowance will be in the range of 2mm to 7mm.

To apply these corrosion rates to account for corrosion over a 20-year service would result in twice the values for the 10 – year service, which is typically an unrealistic approach. An analytical approach to corrosion control could be as follows:

i. Utilize corrosion allowance as a factor of safety for critical items
ii. Plan and implement a corrosion protection system to avoid corrosion wastage.
iii. Develop an appropriate plan to ensure correct and consistent coating maintenance and anode retrofitting.

As established in previous research (Adrien, 2004, Xia, 2013 & Ramesh) a best practice in FPSO maintenance is to avoid wastage due to corrosion by use of adequate means of corrosion protection. This approach eliminates provision of corrosion allowance, although the use of a corrosion allowance on a 10-year service basis or any random value may come in as a safety factor in the design. 2mm for a one-sided exposure applied as a safety factor for critical structural members exposed to corrosive conditions.

The coating of oil and gas production facility which began at the inception of offshore oil and gas production was basically a vinyl or chlorinated rubber-based coating system Production facilities exposed to the atmosphere were treated with multiple coats with a total build of 250-300 microns (10-12 mils). Inorganic zinc silicate primers were incorporated into the systems over time as was epoxy intermediate coats. These proved to be effective for decades and inorganic zinc/epoxy/urethane systems are still used today. Underwater and splash zones were protected with 12-20 mils of coal tar epoxy, thick enough for the system. Another efficient coating that has been used is Hull under water: Six coat system (865 µm total thickness) as follows:

Epoxy primer – 40 µm
Glass flake epoxy – 2 coats x 150 µm/coat
Coal tar epoxy – 75 µm
Self-polishing copolymer anti fouling system – 3 coats x 150 µm/coat (US Department of Transportation, 2014)

The selection and choice of coating system for oil and gas production facilities like the FPSO is guided by the factors such as - Oxygen permeability, water vapour permeability, liquid water uptake, ionic permeability, coating porosity, surface contamination and surface profile (Factors Affecting Coating Lifetime, 2017). In recent years, modern technologies have been used to achieve coatings that meet this satisfy these factors. Organic zinc-rich primers, higher build epoxies, and polysiloxane coatings are among these. However, the major driver for the transition to organic zinc-rich primers (predominantly epoxies but also moisture cure urethanes) is cost and schedule considerations. Organic zinc primers are less expensive than zinc silicates and they are applicable under a broader range of environmental conditions. The higher build formulation typically had lower Volatile Organic Compound (VOC) and Reclaimed Asphalt Pavement (RAPs) than more solvent-laden counterparts. Fewer coats are required to achieve adequate thickness along with film build around sharp edges. Polysiloxane coatings are formulated to provide a durable surface that is resistant to abrasion, wear, and weathering. These properties like the factors that affect lifetime of coatings are critical to durable coating.

Recently there has been some use of thermal spray aluminum (TSA) coatings on offshore structures. TSA can be a high-performance coating system but does not appear suitable for all areas of the structure. Specifically, in immersion areas, the TSA will act as an anode and sacrifice itself to protect exposed steel. Even at thick builds of 10-15 mils, the sacrificial action will quickly consume the TSA coatings, leaving bare steel. The bare steel left behind increases the galvanic reaction on the remaining TSA.

Corrosion of offshore structures results in a significant operational cost to the operators and/or owners of the structures, especially as the structures age (Ramesh, 2014; Ault, 2006). An assessment of the relative effectiveness as well as costs is central to investment decisions concerning life extension and integrity management for older structures. Minerals Management Service (MMS) recognizes the importance of corrosion and corrosion control as part of the overall maintenance effort. It has been identified that 3 forms of corrosion affect FPSOs – General corrosion, Pitting Corrosion such as in-line pitting attack and Grooving corrosion, and Galvanic corrosion (Adrien *et al.*, 2004.

Flares have been identified as having effect on the surrounding perimeter where they are mounted. Anomohanran (2015) reported a drop in temperature from the investigated flair point on a factor of 0.06 °C/m and 0.012 °C/m during rainy and dry seasons respectively. This explains the cause of the degradation of coatings on the Hull of an FPSO with gas Flaring facility. The heat radiation from the flare point affects the coatings on the Hull of an FPSO.

This research is an investigation into the effect of the artificial metocean conditions created by the flare system on the hull of an FPSO. In conducting the study, only metocean conditions associated with thermal radiations from medium pressure (MP) and high pressure (HP) flare systems shall be considered. Other pressure regimes are not covered in this research. Investigation of other parts of the FPSO with respect to thermal radiation effect, other than the hull, is not covered by this work. Although Epoxy generic type products represent a wide range of coatings which are suitable for both new building and for maintenance application, this research considers only Marine Epoxy (Aluminium), Marine Epoxy (Bronze), Epoxy Top-Coat (off Blue), Epoxy Top-Coat (Blue), Poly-urethane paint, Vinyl paint, and Zinc-rich paint for treatment with the listed thermal radiation levels.

This investigation seeks to identify the artificial metocean condition and develop a coating system and formulation that ensures efficient inhibition of the hull of an FPSO in a marine environment exposed to gas flare condition leading to the elimination of frequent shutdown resulting in loss of production, assurance of FPSO hull coating design life, elimination of the huge financial penalties associated with hull maintenance before the expiration of design life and application of coating best suited for the operational environment.

## 2. MATERIALS AND METHODS:

### 2.1 Materials

Materials used in this study include but not limited to DNV PHAST Software, Primary data - real process data from oil and gas facilities, data from FPSO and a personal computer. Since this research is ongoing other materials will be used and these include Sea water, Carbon steel composed of 14% Carbon, 2% Silicon, 40%

Manganese 17% Sulphur, and 12% Phosphorus. Temperature gauge, Thermostatic water bath, 1,000Kw heating Filament, electric power source, pH measuring reagent and coating resins.

## 2.2 Methods

The primary task was the determination of the exposure temperatures to which the coupons are to be subjected. This was accomplished by the use of a DNV PHAST software. Prior to the simulation, the following design data related to the heat sources (flare stacks) were gathered.
Table 1, Process Plant "E" Flare Stack
Design Basis

The environmental requirements for performing reliable simulations are presented on the Tables 2 and 3: Simulations are usually based on very complex equations involving numerous variables too cumbersome to be solved manually. The equation for modelling the heat energy producing the thermal radiation is given by

$$W_{surface} = \frac{F_s m H_{COMB}}{A} \qquad (1)$$

Where:
$F_s$ = Fraction of heat radiated from the surface of the flame [-]
m = Mass discharge rate [kg/s]
$H_{COMB}$ = Heat of combustion of the fuel mixture [j/kg]
A = Total surface area of the flame (conical frustum) [$m^2$]

The simulated thermal radiation-distance results specific to this research are presented in Figure 1 and 2
Thermal radiations cannot be used to treat coupons directly and must be transformed into temperatures for direct application. The correlation between the two parameters is given by Stafan Boltzman's equation (2) as shown below

$$T = \left(\frac{Q}{\varepsilon \sigma A}\right)^{1/4} \qquad (2)$$

Where
T = the absolute temperature (K or °R),

$$\sigma = 5.67 \text{ x } 10^{-8} W/\left(m^2.K^4\right) \left[0.173 \times 10^{-8}\ Btu/(hr - ft^2 - {}^o R^4)\right],$$

$\varepsilon$ = the emissivity of the body, and
A = the body surface area.
Q = Radiation emitted
Combining equation (2), Figure (1) and (2) readily produces two temperatures of 102.4°C and 123.9°C associated with the flare stacks.

Twenty-four (24) flat, hot-rolled steel panels from the same batch of steel and having dimensions of (60 x 40 x 2.0) mm will be grit blasted to a white-metal finish with a roughness profile of 50-70 µm. The number of plates is based on the replications for a $2^3$ factorial experiment. After grit-blasting, each panel will be individually wrapped in moisture resistant paper, which will not be removed until the panel is coated. Three commercial, one-part powder epoxies commonly used for coating FPSO hulls will be used.
A water bath measuring (1700x700x340) mm will be used in holding the test solution. The temperature of the solution will be maintained and regulated by a thermostat-operated 1,500 Kw fillament. Power will be supplied by combining local grid and power generating set.
The coatings will be prepared from predominantly Marine Epoxy, Epoxy, Polyurethane, Vinyl, and Zinc-based paints.

The steel panels are randomly assigned to eight treatment groups; each group will be coated with the three epoxy coatings under investigation. The coatings will be applied to the substrate using a customized line of a rebar coating plant. During this process, the steel panels will be electrostatically sprayed with the powder coating. The thickness of the coatings, which will be controlled by the number of times the electrostatic gun passes over a panel, will be measured at five locations on each panel using a thickness gauge. Only panels falling in the 92-152 ± 10 µm and 150-270 f 25 µm thickness ranges will be used. Coated panels will be tested for holidays using a 67.5 V holiday detector; panels containing holidays will be excluded from the study.

**Table 1: Process Plant "E" Flare Stack Basis**

| Flowrate (MMSCFD) | Gas | Inlet Pressure (bara) | Inlet Temperature (°C) | Flare Tip Diameter (inch.) | Flare Stack Height (m) |
|---|---|---|---|---|---|
| 11.53 | Methane | 3.5 | 65 | 24 | 15 |

**Table 2: Process Plant "O" Flare Stack Design Basis**

| Flowrate (kg/hr) | Gas Data (%) | Inlet Pressure (bara) | Inlet Temperature (°C) 115 | Flare Tip Diameter (inch.) | Flare Stack Height (m) |
|---|---|---|---|---|---|
| 288,664 | $N_2$:0.12 $CO_2$: 1.49<br>Methane: 87.09<br>Ethane: 6.20<br>Propane: 3.18<br>i-C4: 0.73<br>n-C4: 0.75<br>i-C5: 0.07<br>n-C5: 0.06 | 1.5 | | 35 | 50 |

**Table 3: Definition of Pasquill Stability Classes**

| Stability Class | Description |
|---|---|
| A | Extremely unstable conditions |
| B | Moderately unstable conditions |
| C | Slightly unstable conditions |
| D | Neutral conditions |
| E | Slightly stable conditions |
| F | Moderately stable conditions |
| G | Extremely Stable |

Coated panels will be exposed to a test solution containing 30628.00mg/L Chloride, 0.41mg/L Fluoride, 58.00mg/L Sulphate, 3264mg/L Calcium and traces of other elements characteristic of the operating environment being simulated. This solution is typical of the marine environment to which the FPSO hull is exposed. All of the panels assigned to the corrosion experiment will be immersed in the test solution heated between 102.4°C and 123.9°C with all other factors such as pH and salinity adjusted between their low and high levels as required in designed factorial experiments. Wet adhesion test will be conducted at atmospheric conditions only. In all phases of the experiments, the solution will continuously be aerated by bubbling filtered and desiccated exposing the water bath with content to the atmosphere and stirring the solution periodically. The salinity, pH, and temperature of the solution will be measured periodically.

### 2.2.1 Quantification of degradation of Coatings by Gravimetric Measurement

The gravimetric (weight loss) measurement will be carried out using standard methods and as reported by Izionworu *et al*. (2021) and Oguzie *et al*. (2010) to determine the corrosion rate (Cr), surface coverage (θ), and inhibition efficiency (IE%) using Equations (3), (4) and (5).

$$\text{Cr (mmy-1)} = {}^{87{,}600\Delta W}/_{\rho At} \qquad (3)$$

Where: W is the average negative change in weight (g), (**$\rho$**) is the carbon steel density (g/cm3), A is the surface area of the coupon and t is the immersion time and 87,600 is the conversion constant from cm h-1 to mm y-1.

The expression of equations 4 and 5 also reported by Izionworu, *et al., 2021 and* Yadav, *et al.*, 2015:

$$\theta = \left(1 - \frac{C_r^{ihb}}{C_r^{blk}}\right) \qquad (4)$$

$$\text{IE\%} = \left(1 - \frac{C_r^{ihb}}{C_r^{blk}}\right) \text{ x } 100 \qquad (5)$$

Where ϴ is the surface coverage, ($C_r^{blk}$) is the coupon corrosion rate in the blank corrodent solution, ($C_r^{inh}$) is the rate of the coupon corrosion in the presence of inhibitor in the corrodent solution. IE% is the inhibitor efficiency.

The test will be in a thermostatic water bath that shall be maintained for temperature test between 102.4°C and 123.9°C**.**

### 2.2.2 Identification and Characterization of the Active Compounds of the Extracts

To identify and characterize the coating degradation Fourier Transform Infrared Spectroscopy and Gas Chromatography-Mass Spectrometry (GC-MS) will be used. The coatings $S_1$ and $S_2$ to FTIR analysis and report obtained with GC-MS FTIR MODEL IS-630 Cary Series by Agilent Technologies spectrophotometer at a frequency of 4000 to 400 cm-1. The spectra for the coating under investigation, as well as the protective film observed on the surface of the carbon steel after every 5 days of immersing the coupons in seawater environment, will be recorded by carefully removing the coating and making the pellets, this is as reported by Ramesh et al. (2001), and Shylesha *et al.* (2011).

Sample for Gas Chromatography analysis will be analyzed using the Agilent 6890 gas chromatograph with a 5973 MS detector equipped with 60 m x 0.25 mm, i.d. 0.25

µm/MS DB-WAX capillary column (Agilent).. Also, the phytochemical composition of each sample ($S_1$ and $S_2$) will be identified with Agilent 6820 gas chromatograph. The mass spectrum results will be interpreted using the database of the National Institute Standard and Technology (NIST) having more than 62,000 patterns. The fragmentation pattern spectra of the unknown components will be compared with those of known components stored in the NIST V. 3.2 library.

### 2.2.3 Determination of Electrochemical measurement parameter

The electrochemical polarization test shall be carried out using a PARSTAT-2273 Advanced Electrochemical System with Power suit software in a conventional three-electrode configuration in which graphite rod served as counter electrode and the reference electrode shall be the saturated calomel electrode (SCE) and working electrode shall be mild steel that has the compositions mentioned earlier. The Potentiodynamic polarization investigations shall be conducted in a potential range ±250 mV versus corrosion potential, at a scan rate of 0.333mV/s, in aerated and unstirred solutions at the end of 5, 10, 15, 20, 25 and 30 days of immersion at test temperatures. Each test shall be repeated three times to make sure they are reproducible.

The values of the corrosion current density in the absence ($I_{corr,bl}$) and presence of inhibitor ($I_{corr,inh}$) were used to estimate the inhibition efficiency (IE%) from polarization data using equation (6).

$$IE\% = \left(\frac{I_{corr(bl)} - I_{corr(inh)}}{I_{corr(bl)}}\right) x\ 100 \qquad (6)$$

where $I_{corr(bl)}$ and $I_{corr(inh)}$ respectively represents the current density of the corrosion system without the coatings. (Izionworu, *et al.*, 2020; 2021 & 2022; Wang *et al.*, 2011).

### 2.2.4 Scanning Electron Microscopy Studies of the Effect of CVB-WC on Mild Steel

Morphological investigations of the surface of the carbon steel after immersion in the simulated environment solution with and without the coatings shall be undertaken by SEM examinations of the surfaces exposed to the different test solutions using XL-30FEG scanning electron microscope. The carbon steel coupons from the test environment will be examined after 5, 10, 15, 20, 25, and 30 days of exposure will be subjected to SEM investigative (Oguzie *et al.*, 2007).

### 2.2.5 Holiday Detection Methods

Fully cured, coating will be tested for holidays using the two main holiday detection methods; the first being the Wet Sponge Method, the second being the more widely used High Voltage DC Method. The general rule of thumb within the industry will be applied, that is 4 volts per micron of material being tested.

## 3.0 RESULTS AND DISCUSSION

The thermal radiation levels simulated using DNV PHAST Software for the two flare stacks are (3.9Kw/m$^2$ and 4.1Kw/m$^2$) from systems operating at 3.5 bara and 1.5 bara respectively. The establishment of these thermal radiation values are very important for two reasons. First, they indicate the exposure levels of field operators to heat hazards (NIOSH, 2016). High thermal radiation levels could cause excessive dehydration and death. Secondly, these values provide the basis for regulatory organizations to monitor operators' activities to ensure that they are within regulatory limits. These thermal radiation levels and their associated pressure regimes are shown in Table 4.

**Table 4: Thermal Radiation and Temperature Values for Flare Stack "O" and "E"**

| Parameters | Flare Stack "O" | Flare Stack "E" |
|---|---|---|
| Inlet Pressure (bara) | 1.5 | 3.5 |
| Thermal Radiation (Kw/ $m^2$) | 4.1 | 3.9 |
| Temperature ($^0$C) | 102.43$^0$C | 123.85$^0$C |

It is extremely important that process plant designers, owners, and operators are aware of how thermal radiations are distributed in relation to distance upwind and downwind. These distribution curves are essential in decision-making during equipment layout during onshore/offshore development projects. Figures 1 and 2 present the thermal radiation-distance curves for flare stack "O" and "E".

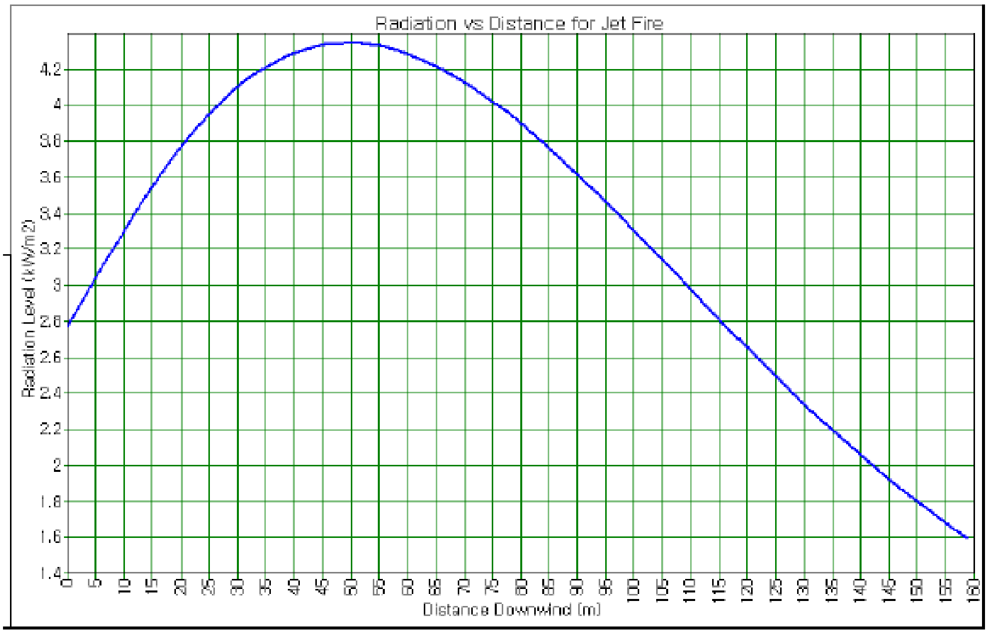

**Figure 1: Radiation Level vs Distance (at 21 m/s of wind speed) for "O"**

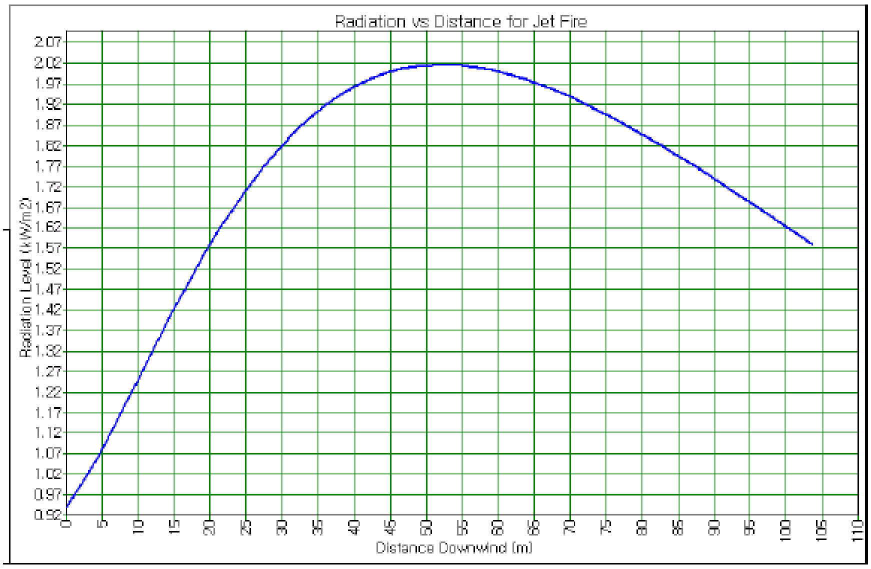

**Figure 2: Radiation Level vs Distance (at 21 m/s of wind speed) for "E"**

## 4.0 CONCLUSION

The thermal radiations associated with the two-flare stack have been successfully modelled. The temperatures corresponding to these thermal radiation levels have also been calculated from Stefan Boltzman's equation. Factorial experiment shall be performed to investigate how three coatings ($S_1$ , $S_2$ and $C_c$ ) for the hull of FPSO will respond to treatment from a combination of temperature, salinity, and pH. It is expected that the superiority or inferiority of $S_1$ and $S_2$ to $C_c$ shall be fully established and designers during FPSO construction projects can then make the right decisions relating to coating design for FPSO hull protection to minimize downtime and production losses.

## REFERENCES

Adrien, M., Karl, P.F., Henning, C., Oystem, G. & Det, N.V. (2004). Newbuild FPSO Corrosion Protection – A design and Operation Planning Guideline. Prepared for Offshore Technology Conference, 1-11. Retrieved from https://www.scribd.com/document/448886850/Newbuild-FPSO-Corrosion-Protection

Anomohanran, O. (2015). Evaluating the Thermal Impact of Gas Flaring in Kokori, Southern Nigeria. *Applied Physics Research*, 7(1), 78-83.

Coatings for Corrosion Protection: Offshore Oil and Gas Operation Facilities, Marine Pipeline and Ship Structures" (2004). United States Department of Transportation -- Publications & Papers. 6. https://digitalcommons.unl.edu/usdot/6

Factors Affecting Lifetime of Corrosion Protection Coatings (2017, May 22). Retrieved from https://www.sealxpert.com/factors-affecting-lifetime-of-corrosion-protection-coatings/

Farag A. A., Ismail, A. S., & Migahed, M. A.

(2015). Inhibition of Carbon Steel Corrosion in Acidic Solution Using Some Newly Polyester Derivative. *Journal of Molecular Liquids* 211, 915-923

Izionworu, V. O., Oguzie, E. E. & Amadi, S. A. (2020). Electrochemical, SEM, GC-MS And FTIR Study Of Inhibitory Property of Cold Extract of Theobroma Cacao Pods For Mild Steel Corrosion In Hydrochloric Acid. *International Journal of Engineering Trends and Technology* 68(2), 82-87.

Izionworu, V.O, Puyate, Y.T. & Wan-Nik, W. M.N. (2021). A Study of Wire Croton as an Inhibitor of Mild Steel in HCL Using Electrochemical – SEM – GCMS and FTIR Measurements. *Journal of Newviews in Engineering and Technology*, 3(1), 1-11.

Izionworu, V.O., Said, B., Arukalam, I.O. & Wan Nik, W.M.N. (2022). Inhibitive Mechanism of Acid Corrosion of Cold-Rolled Steel by Polyethylene Glycol via Experimental, Computational and Surface Analytical Approaches. *Journal of Bio- and Tribo-Corrosion*, https://doi.org/10.1007/s40735-021-00613-5.

John, P. (2013). FPSO Design: Hull, Accommodation, Mooring, Turrets, and Risers.

Johnson Komboye, (2014). Enhancing Vortex Induced to Harness Hydrokinetic Energy from Ocean/River Current for Electricity Generation.

Melchers, R.E., Jeffery, R. & Fontaine, E. (2012). Corrosion and the structural safety of FPSO Mooring Systems in Topical Waters. Proceedings of the OTC Retrieved from, https://www.yumpu.com/en/document/read/32363759/corrosion-and-the-structural-safety-of-fpso-mooring-asec2012

NIOSH [2016]. NIOSH Criteria for a Recommended Standard: Occupational Exposure to Heat and Hot Environments. U.S. Department of Health and Human Services, Centers for Disease Control and Prevention, National Institute for Occupational Safety and Health, DHHS (NIOSH) Publication 1 - 192.

Oguzie, E. E. (2007). Corrosion inhibition of aluminum in acidic and alkaline media by Sansevieria trifasciata extracts. *Corrosion Science*, *49*, 1527-1539.

Oguzie, E. E., Enenebeaku, C. K., Akalezi, C. O., Okoro, S. C., Ayuk, A. A., & Ejike, E. N. (2010). Adsorption and Corrosion inhibiting effect of Dacryodis edulis extract on low carbon steel corrosion in acidic media. *Journal of Colloid Interface Science*, *349*(283).

Ozgur O., (2021). Conversion of an oil tanker into FPSO in Gulf of Mexico: strength and fatigue assessment, Ships and Offshore Structures. *Ships and Offshore Structures*,16(9), 993-1011, DOI: 10.1080/17445302.2020.1790298

Pike, W.J. (199). Economic Benefits of FPSO Construction and Deployment in the Gulf of Mexico. Paper presented at the Offshore Technology Conference, Houston, Texasdoi: https://doi.org/10.4043/11001-MS

Ramesh, S. (2014). Corrosion Control for Offshore Structures. (1st ed). Waltham, MA 02451, USA. Elsevier Inc.

Ramesh, S. P., Vinod Kumar, K. P., & Sethuraman, M. G., (2001). Extract of *andrographis paniculata* as corrosion inhibitor of mild steel in acid medium, *Bulletin of Electrochemistry*, 17, 141–144.

Shylesha, B. S., Venkatesha, T. V., & Praveen, B. M. (2011). Corrosion inhibition studies of mild steel by new inhibitor in different corrosive medium. *Research Journal of Chemical Sciences*, 1(7), 46-50.

Yadav, M., Sinha, R. R., Sarkar, T. K., Bahadur, I., & Ebenso, E. E. (2015). Application of New Isonicotinamides as a Corrosion Inhibitor on Mild Steel in Acidic Medium: Electrochemical, SEM, EDX, AFM and DFT investigations. *Journal of Molecular Liquids*. 212, 686-698.

Xia, J. (2013). FPSO Design to Minimise Operational Downtime due to Adverse Metocean Conditions off North West Australia. *Deep Offshore Technology*, 27-29. Perth, Australia